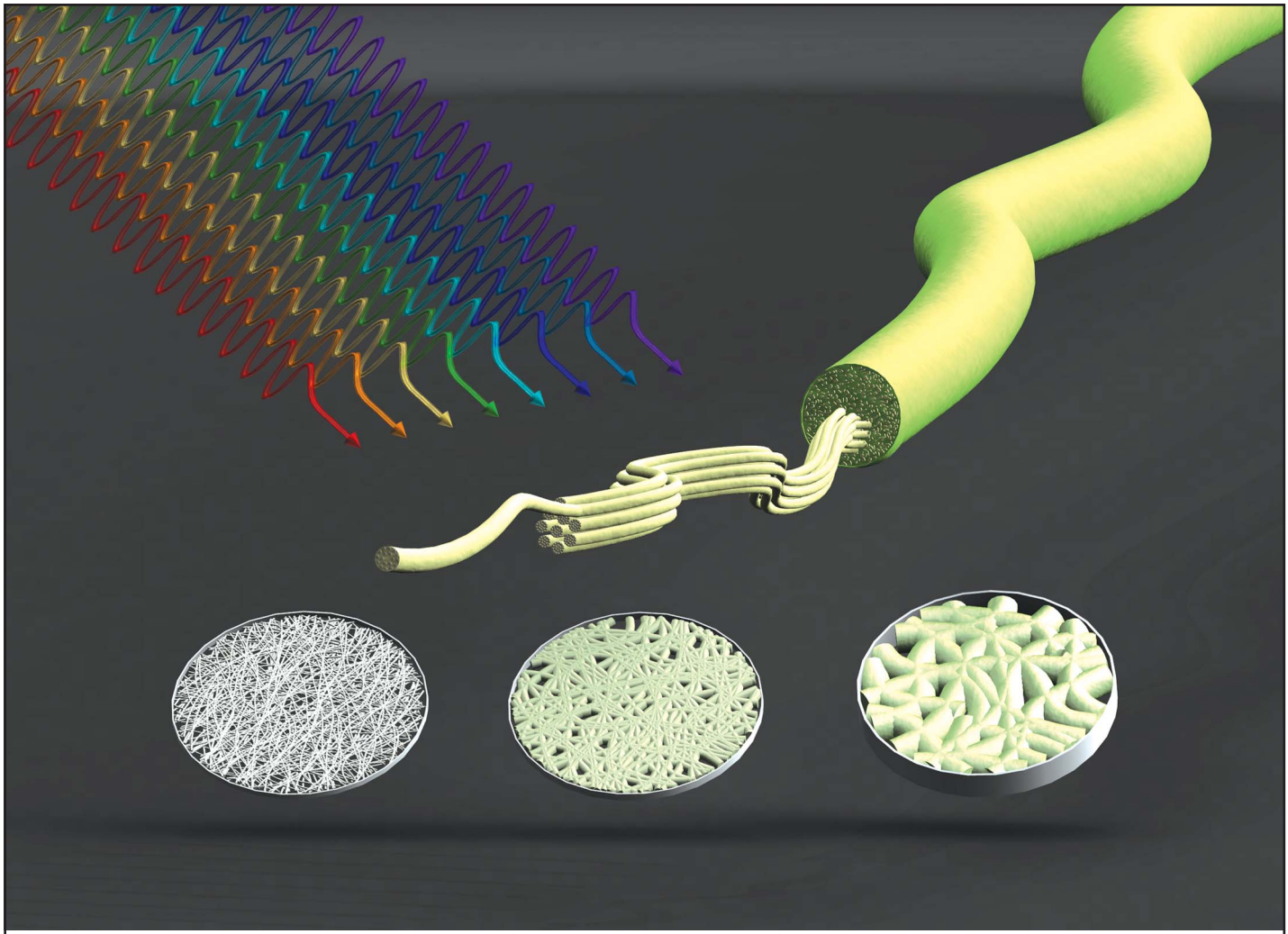

Showcasing research from the Department of Materials Science and Engineering, University of Maryland, United States.

Title: Transparent nanopaper with tailored optical properties

Nanopaper based on biodegradable cellulose fibers with tailorable optical properties shows a strong dependence on the cellulose fiber diameter and packing density. The optical properties are thoroughly explained through Chandrasekhar radiative-transfer theory and multiple scattering method simulations. The controllable optical properties of the highly transparent nanopaper present an unprecedented opportunity for the growth of next-generation optoelectronics.

As featured in:

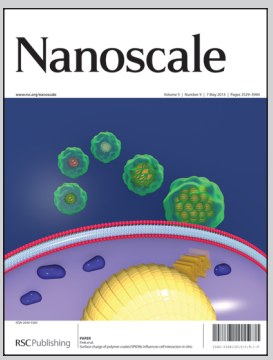

See Hu *et al.*, *Nanoscale*, 2013, **5**, 3787.

RSC Publishing

www.rsc.org/nanoscale

Registered Charity Number 207890

Nanoscale

RSC Publishing

PAPER

View Article Online
View Journal | View Issue

Cite this: *Nanoscale*, 2013, **5**, 3787

Transparent nanopaper with tailored optical properties†

Hongli Zhu,[a] Sepideh Parvinian,[a] Colin Preston,[a] Oeyvind Vaaland,[b] Zhichao Ruan*[c] and Liangbing Hu*[a]

Received 29th January 2013
Accepted 25th February 2013

DOI: 10.1039/c3nr00520h

www.rsc.org/nanoscale

Nanopaper is a flexible, transparent, and renewable substrate that is emerging as a replacement for plastic in printed "green" electronics. The underlying science of transparency of nanopaper is that the diameter of these fibers is much smaller than the light wavelength, which significantly decreases the light scattering as compared to regular fibers. Cellulose fibers have a hierarchical structure, which consists of numerous smaller fibers. In this manuscript, we demonstrate a nanopaper design with different fiber diameters, and conclude that the light transmittance and scattering depend on the fiber diameter and packing density. The optical properties of the nanopaper and their dependence on the cellulose fiber diameter are thoroughly explained through Chandrasekhar's radiative-transfer theory and multiple scattering method simulations. The controllable optical properties of highly transparent nanopaper present an unprecedented opportunity for growth of next-generation optoelectronics.

1 Introduction

Flexible plastic substrates are ubiquitous in electronic devices because of their excellent mechanical properties, lightweight, roll-to-roll processing capability, and low cost. Plastic substrates already host high performing devices such as organic solar cells, light-emitting diodes, transistors, and circuits.[1–4] Typical flexible substrates are polyethylene terephthalate (PET), polyethylene naphthalate (PEN), and polycarbonate (PC). Although plastic substrates have certainly achieved success in a variety of devices, they carry several disadvantages that drive a need to replace them in certain applications. For example, plastic substrates possess a low coefficient of thermal expansion (CTE) and processing temperature, and in some cases are not renewable for based on petrochemistry.[5] Plastic substrates are also inferior to paper substrates for roll-to-roll printing. Extra additives are needed to enable an ink to be printed on a plastic substrate. Paper has attracted much attention as an emerging substrate for flexible electronics.[6–10] A traditional wood fiber has a unique hierarchical structure; a large fiber with diameter ~25 μm is made of many small fibers (microfibrils), each composed of many protofibrils (elementary fibrils).[11] The cellulose fiber diameter must be smaller than the optical wavelength to achieve a high optical transparency.

Transparent nanopaper is an emerging substrate for electronics,[7,12] and is more flexible and more printable than plastic. It also possesses a better CTE than plastic and stability at higher temperatures.[13] Common paper is made of cellulose fibers with an average diameter of ~25 μm, which induces significant light scattering that results in an opaque substrate. The larger fiber diameter also leads to a rough surface, which is incompatible with electronic devices composed of layers typically 100 nm thick. The regular fibers can be disintegrated into smaller fibers with a diameter reduced to tens of nanometers and a length to several micrometers by controlling the processes such as the pretreatment time, chemical dosage, and numbers of microfluidizer treatment.[14,15] Our group primarily focuses on the optical properties of transparent nanopaper, in particular the relationship between fiber geometry and light scattering. The light management of transparent substrates is extremely important for optoelectronic devices. For example, an increased absorption path of light in a solar cell will enhance the device's conversion efficiency, thus a considerable light scattering is preferred.[16,17] Light scattering, however, will cause an optical haze effect that is detrimental for indoor displays. An anti-glare coating is needed for display driven devices to function in bright environments, such as for touch screens in global positioning systems (GPS).[18] For such applications, an anti-glare coating with large light scattering is required. It is very important, therefore, to be able to tailor the light scattering of the transparent substrates for different applications.

In this paper, we describe the optical properties of transparent nanopaper with different fiber diameters. Specular

[a]*Department of Materials Science and Engineering, University of Maryland, College Park, MD 20742, USA. E-mail: binghu@umd.edu*

[b]*Department of Mechanical Engineering, University of Maryland, College Park, MD 20742, USA*

[c]*Department of Physics, Zhejiang University, Hangzhou, Zhejiang 310012, China. E-mail: zc.ruan@gmail.com*

† Electronic supplementary information (ESI) available. See DOI: 10.1039/c3nr00520h

transmittance, diffusive transmittance, and haze are evaluated for transparent nanopapers. We focus on two important parameters to tailor light scattering in transparent nanopaper: the fiber diameter and the packing density. We conclude that the total diffusive transmittance does not vary much as the fiber diameter is reduced from 50 nm to 10 nm, however specular transmittance and the haze values change dramatically in the visible wavelength range. The packing density can also significantly alter the diffusive transmittance. We also show that the Chandrasekhar radiative transfer model used to describe the light transport in random turbid systems fits our experimental data. We use the multiple scattering method to simulate the impact of fiber diameter on the light scattering by nanopaper. The ability to tailor the optical properties of transparent nanopaper is critical for further applications of this emerging biodegradable flexible substrate towards next-generation optoelectronics.

2 Results and discussions

2.1 NFC disintegration and nanopaper fabrication

Wood fiber is a sustainable material with an intrinsic hierarchical structure. The size of natural fibers in softwood is around 20 μm to 40 μm in diameter and 1–3 mm in length. A single fiber is obtained by delignification treatment; this includes chemical cooking/bleaching and mechanical grinding/screening. The obtained fiber is composed of more than 90% cellulose and small amounts of hemicellulose. As shown in Fig. 1(a), one common fiber is composed of thousands of microfibers, each composed of element fibrils.[13,19] Common cellulose fibers can be disintegrated into smaller sizes with a combination of mechanical and chemical treatment. The never-dried softwood fibers are oxidated with TEMPO ((2,2,6,6-tetramethylpiperidin-1-yl)oxidanyl), which is a highly selective oxidant for the hydroxymethyl group at the glycose C6 position in the cellulose chain to a more active carboxyl group.[19,20] The TEMPO treatment is in an aqueous system. Cellulose swells by generating a negative charge, which enables production of nanofibrillated cellulose (NFC) following a final microfluidizer treatment. The ultimate fiber diameters vary from 10 nm to a few hundred. Nanopaper was fabricated with a vacuum filtration process, then pressed and dried in air. The pressure and drying temperature controls the density of the nanopaper. The concentration of the NFC gel is typically ~1% by weight and the hydrocolloid dispersion is stable at a ζ potential of −75 mV.[20] Our group disintegrates the fibers at different levels and fabricates papers with different transmittances. Fig. 1(b) shows the paper made from regular fibers with an average diameter of 25 μm, which does not form a transparent substrate. As the fiber diameter decreases to 50 nm and 10 nm, the nanopaper becomes more and more transparent (Fig. 1(c) and (d)).

Diluted and stabilized cellulose dispersions were fabricated to investigate the dependence of light scattering on the fiber diameter. The concentration of the dispersion is held the same: 1 mg mL^{-1}. A laser beam with a wavelength of 650 nm was directed incident from the left of the bottle, as shown in Fig. 2(a). Light scattering within the solution visibly progressed as the fiber diameter increased (a bottle of pure water is used as the reference). Scanning electron microscopy (SEM) and atomic force microscopy (AFM) were used to measure the fiber dimensions. The average wood fiber has a diameter of ~25 μm (Fig. 2(b)). The shape of dried fibers is not perfectly round. To measure the diameter of the nanofibers, the dispersion is deposited on a plasma treated Si substrate. Fig. 2(c) and (d) show the AFM images of cellulose networks with a fiber diameter of 50 nm and 10 nm, respectively. Nanofibers with tunable fiber diameters are excellent building blocks for engineering the next-generation of transparent substrates with tailored optical and mechanical properties.

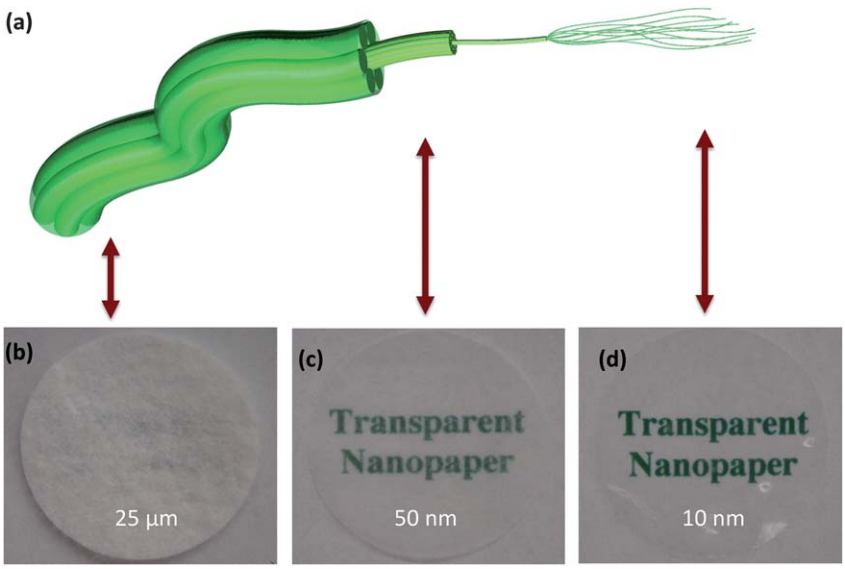

Fig. 1 (a) Schematic of the hierarchical structure for cellulose fibers. (b–d) Cellulose paper made of fibers with three different diameters, 25 μm, 50 nm and 10 nm. The paper thickness is the same, 40 μm. As the fiber diameter decreases, the optical transmittance increases.

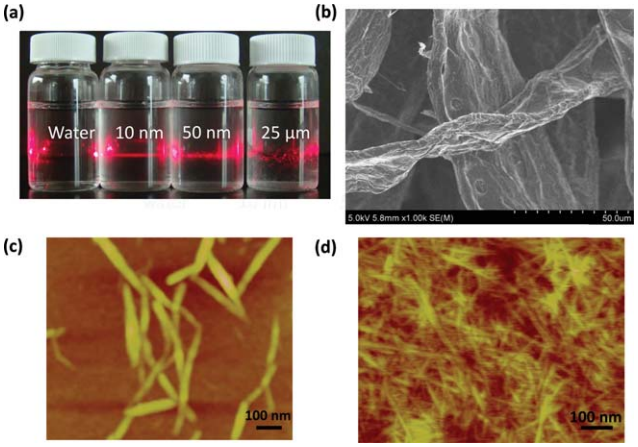

Fig. 2 (a) An image of various cellulose dispersions under light illumination. The left bottle contains no cellulose. A horizontal laser light is incident from the left side with regard to the viewing perspective. As the fiber diameter increases, the light scattering in the dispersion increases. (b) SEM image of 25 μm fiber. (c) AFM height image of cellulose fibers with 50 nm diameter. (d) AFM height image of cellulose fibers with 10 nm diameter.

2.2 Effect of fiber size and packing density to nanopaper's optical properties

The light scattering of individual cellulose fibers perpetuates the collective optical properties of nanofiber substrates. These fibrous building blocks with little light scattering leads to a unique behavior of light, which is advantageous for several applications. There are two kinds of transmittances: specular transmittance and diffusive transmittance. For specular transmittance (Fig. 3(a)), the photo-detector only measures the light flux that transmits along the same axis as the incident flux. For diffusive transmittance, the transmitted light is collected at all angles by an integrating sphere. The difference between the diffusive and specular transmittance gives the total forward scattering. The measurement was done for paper substrates, as shown in Fig. 1. The data for fiber diameter of 25 μm, 50 nm and 10 nm are shown in Fig. 3(b)–(d), respectively. The paper in Fig. 3(b) is made from the fiber presented in Fig. 2(b), which has a low specular transmittance (37%) and a low diffusive transmittance (5%) at 550 nm wavelength. For the nanopaper made from 50 nm cellulose fibers (Fig. 3(c)), the transmittance is reduced from 92% to 19% after removing the integrating sphere. In Fig. 3(d), nanopaper made from 10 nm NFC has a diffusive transmittance of 93% and a specular transmittance of 71%.

For fibers with diameters of 50 nm and 10 nm the optical transmittance reaches up to 92–93%, which is higher than a plastic substrate with the same thickness. The optical transmittance for nanopaper with these two diameters is very similar, but the light scattered off the normal direction is much higher for fibers with a 50 nm diameter than for a 10 nm diameter. This enables an important possibility to tune the optical properties of nanopaper to benefit different applications. Nanopaper with a fiber diameter of 50 nm is more suitable for solar cell applications, because the high degree of scattering increases the optical length and thus the light absorption in the active layers of solar cells. The increased

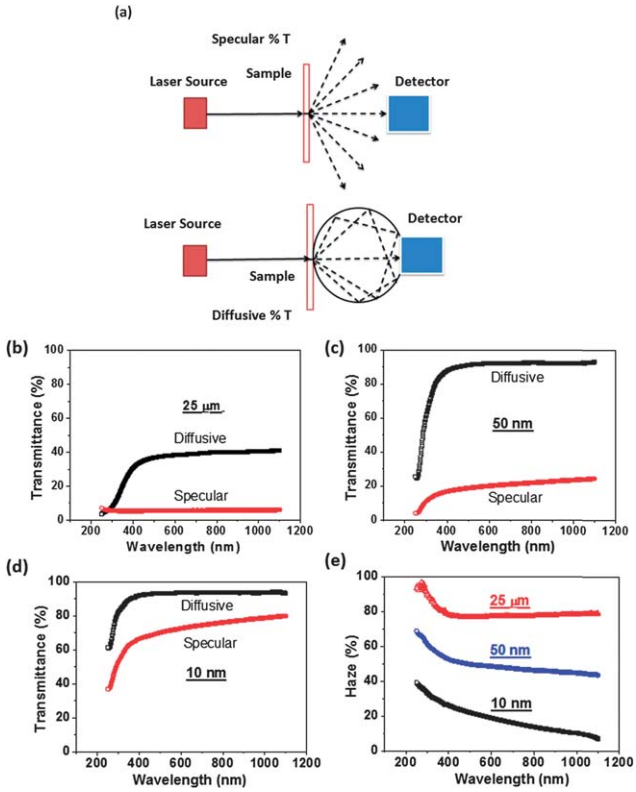

Fig. 3 (a) A schematic to illustrate the specular and diffusive transmittance. (b–d) The specular and diffusive transmittance for paper with fiber diameters 25 μm, 50 nm, and 10 nm, respectively. As the fiber diameter increases, the percentage difference between diffusive and specular transmittance increases. (e) The haze for paper with different fiber diameters. All the papers are fabricated at the same thickness with 40 μm.

adsorption enhances the short circuit current density, which is already reported for solar cells with transparent metal nanowire substrates.[21] Nanopaper with 10 nm diameter fibers is more suitable for indoor displays that require a high clarity. The scattering of nanopaper can also lead to an anti-glare effect, which is widely used in outdoor displays where devices operate in a bright environment.

Optical haze is used to quantify the percentage of the forward light scattering, and is experimentally quantified as:

$$\text{Haze} = \left[\frac{T_4}{T_2} - \frac{T_3}{T_1}\right] \times 100\% \quad (1)$$

where T_1, T_2, T_3 and T_4 are defined in the ESI (Fig. S1†). T_2 is the total (diffusive) transmittance, and T_4 is the forward scattering (*i.e.* total transmittance − specular transmittance). The procedure is described in the ASTM D1003 "Standard Method for Haze and Luminous Transmittance of Transparent Plastics".[22] The paper made from 25 μm, 50 nm, and 10 nm fiber possess a haze value of about 77%, 49%, 20% at 550 nm, respectively. The larger cellulose fibers lead to a larger haze value. Optical haze *vs.* wavelength is plotted in Fig. 3(e). The diameter of the pristine cellulose fibers (25 μm) is much larger than the light wavelength, which causes more than 80% of the total transmittance to be forward scattered off the normal direction. Nanopaper

composed of 50 nm diameter fibers has an optical transmittance reaching up to 92%, approximately 50% of which is contributed from the forward scattering. The optical properties of transparent nanopaper present an unprecedented possibility for the development of optoelectronic devices such as organic solar cells, light emitting diodes, and displays.

In addition to the diameters, the optical properties can also be altered by the packing density of cellulose fibers in paper. When a photon encounters an object it can interact with it *via* reflection, adsorption, or refraction. These interactions depend on the wavelength of light and the properties of material. There are internal pore within the nanopaper. According to Snell's Law, the photon can be scattered at either the interface where there is a change in the index of refraction, or internally. The larger the difference in the refractive index between air and the medium, the more the photons will be scattered. The refraction index of air is around 1.0 and the porous cellulose is around 1.2. The air within the nanopaper's internal layer structure will increase light scattering, and reduce the transmittance. We designed nanopaper with three different packing densities (52 μm, 40 μm and 36 μm as shown in Fig. 4(a)–(c)) using 10 nm NFC, which was achieved by controlling the pressing pressure during the drying process. Each sample's thickness is decreased with increased pressure. As the packing density increases, both the specular and diffusive transmittance increase (Fig. 4(d) and (e)). Note that the total amount of cellulose used for three different nanopaper samples is the same. The packing density reflected by the nanopaper thickness can significantly change the light–cellulose fiber interaction. As the packing density increases, the effective index of nanopaper increases. Meanwhile, the porosity of paper decrease, which decrease the scattering and increase the optical transmittance. The air volume in the pores of nanopaper decreases, however, which decreases the amount of light scattering. The decreased amount of scattering explains the increase of the transmittance and the decrease in the haze value (Fig. 4(f)). Controlling the packing density of nanopaper provides another effective method to tune the optical properties of nanopaper in addition to varying the diameters of cellulose fibers. It is noteworthy that the packing density will affect the flexibility, printability, and barrier properties of nanopaper.[23,24]

2.3 Modeling of fiber size dependent light scattering

The ability to tune the nanopaper transparency and haze *via* the nanofiber diameter can be understood from the scattering behavior of nanofibers. Fig. 5(a) shows the electromagnetic (EM) scattering cross-section of a single nanofiber. Here the simulation was derived from the Mie scattering theory;[25] assuming that unpolarized light illuminates an infinitely long fiber, and the dielectric constant of the porous nanofiber is 1.32.[26] When the fiber diameter is much less than wavelengths in the visible range, the EM scattering cross-section decreases sharply with the nanofiber diameter [Fig. 5(a)], as predicted by Rayleigh's Scattering Theory with $\sigma_{sct} \propto D^3$ where D is the fiber diameter and σ_{sct} is the scattering cross-section. This indicates that the smaller diameter nanofibers lead to a much higher transparency for nanopaper. To illustrate the impact of the nanofiber's diameter on the haze factor of the substrate, we used a multiple scattering method to simulate that an incident plane wave illuminates a bunch of randomly distributed nanofibers.[27] Fig. 5(b) and (c) show the EM field through nanofibers with the same density, but with either a fiber diameter of 25 nm or 50 nm. The illuminating light is incident from the left side with a unitary amplitude and with a TM polarization (the magnetic field is parallel to the axis of nanofibers). As previously described, 50 nm diameter nanofibers lead to about 8 fold larger scattering than 25 nm diameter fibers. The comparison between Fig. 5(b) and (c) clearly shows 50 nm diameter nanofibers have a much stronger twist to the wavefront than 25 nm diameter fibers. The white lines in Fig. 5(b) and (c) correspond to the Poynting vector lines, which present

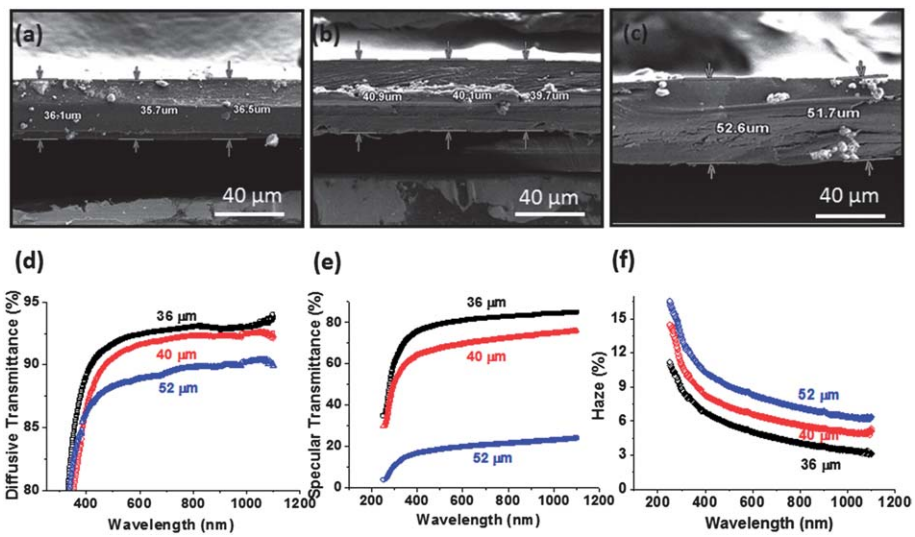

Fig. 4 (a–c) cross-sectional SEM images of papers fabricated with different pressing pressures. The thicknesses are 36 μm, 40 μm, and 52 μm. (d and e) The specular and diffusive transmittance for papers with different densities. (f) The haze value *vs.* the wavelength for nanopapers with different packing densities.

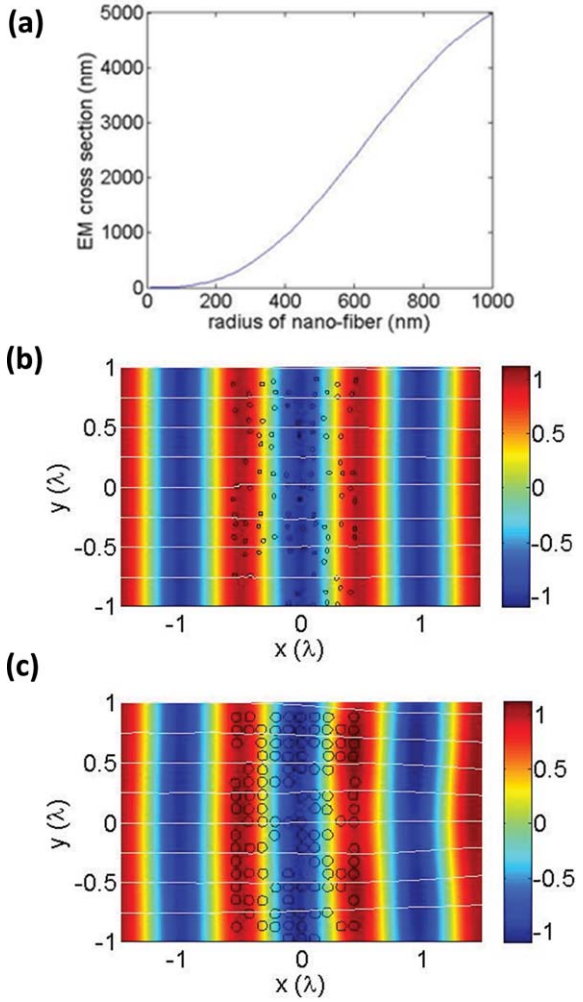

Fig. 5 (a) The EM scattering cross-section of an individual nanofiber *vs.* the fiber diameter. The wavelength for the calculation is fixed at 550 nm, and the scattering cross-section is averaged on the incident angle and polarizations. (b and c) are the total field distributions for a plane wave incident from the left side on a bunch of randomly distributed nanofibers with a diameter of 25 nm and 50 nm, respectively. The white lines correspond to the Poynting vector lines, which present the trajectory of light. The black circles outline the cross-section of nanofibers.

the trajectory of light through the nanofiber bunch. According to the (Poynting) vector lines, the normal incident light is scattered farther off its original axis by nanofibers with larger diameters. This illustrates that increasing the nanofiber diameter leads to higher optical haze in the nanopaper.

For nanopaper, which is the collection of millions of randomly distributed nanofibers, unfortunately the rigorous optical field distribution cannot be calculated because of extreme complexities. The light transmittance through such a turbid medium, however, is empirically modeled by the Chandrasekhar radiative transfer equation.[28] When the fiber diameter is much smaller than the wavelength of the incident light, the scattering is isotropic. In such a case, the Chandrasekhar radiative transfer equation has an analytical form, and the transmission is given as:

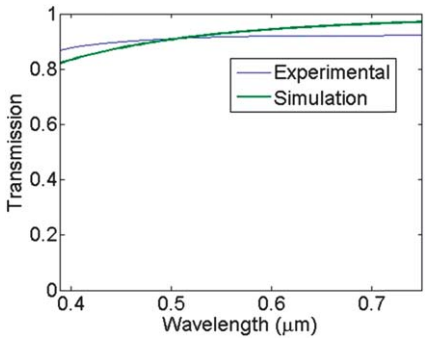

Fig. 6 The optical transmittance in the visible range fits with the Chandrasekhar radiative-transfer model, with $T = \frac{1}{1+\frac{3}{4}\rho\sigma_{sct}h}$ for a pure-scattering case without light absorption, where ρ is the density, σ_{sct} is the scattering cross-section of a single scatter object, and h is the thickness of the slab.

$$T = \frac{1}{1+\frac{3}{4}\rho\sigma_{sct}h} \quad (2)$$

where T is the optical transmittance, ρ is the density, σ_{sct} is the scattering cross-section of a single scatter object, and h is the thickness of the slab.[29] As Fig. 6 shows, we find that the experimental data fit well with the Chandrasekhar radiative transfer model. Here the nanofiber for the measured nanopaper has an average diameter of 50 nm, and the thickness of nanopaper is 40 μm. The only fitted parameter is $\rho = 43\ \mu m^{-2}$, which is appropriate for the experimental sample.

3 Conclusions

We studied in detail the optical properties of transparent nanopaper with different cellulose fibril diameters and packing densities. We conclude that transmittance and haze values can be tailored dramatically with the diameters of the nanopaper fibers. Optical transmittance data are modeled by a theory derived from the Chandrasekhar radiative transfer equation. The diameter dependence of optical transmittance is explained with the scattering cross-section of individual cellulose fibrils. Optical haze reaches up to 50–60% for a nanopaper sample with a total diffusive transmittance of 90%. This is dramatically different from contemporary transparent plastic and glass substrates. The large haze value of transparent nanopaper is extremely useful for certain lighting devices. The light scattering of transparent nanopaper can also increase the light absorption in the active layer of solar cell devices for improved device performance. The tunable optical properties open new opportunities for the device applications of transparent nanopaper.

4 Experimental section

4.1 Disintegration of NFC with different diameters

The ultimate fiber diameters vary from 10 nm to a few hundred nanometers, which can be controlled by the power and processing time. 5 g of Kraft bleached softwood (Southern Yellow

Pine) pulp was suspended in 250 mL of deionized water containing 0.5 mmol of TEMPO and 5 mmol of NaBr. The TEMPO mediated oxidation was instigated by adding 10 mmol of NaClO. The pH was maintained at 10.0 with 1 mol L^{-1} NaOH until no pH reduction was observed. The obtained pulp was washed through a filtration, and stored in a cold environment at 4 °C for further analysis and treatment. The average diameter of the obtained fiber was around 1 μm after the TEMPO treatment. The fiber was then treated with a Microfluidizer (Microfluidizer Processor M-110 EH) under different pressures, with 1.0% aqueous concentration. The 50 nm and 10 nm fiber diameter was obtained at a pressure of 10 000 psi and 26 000 psi, respectively.

4.2 Nanopaper fabrication and characterization

The dispersion was degassed for 20 minutes with a bath sonication under the degas function until no bubble was observed in the suspension. The dispersion was poured into the filter composed of a nitrocellulose ester filter membrane (Millipore DAWP29325) with a 0.65 μm pore size. The filtration time was dependent on the necessary thickness of the nanopaper and the nanosize of NFC. It is more time consuming for smaller fibers due to the presence of higher surface charges. After filtration, a strong gel formed on the top of the filter membrane. The gel "cake" was placed in the 40 °C oven for 10–15 minutes. It was then put in the 105 °C hot press for 10–15 minutes. After drying, a transparent, flexible, and strong nanopaper with a 90 mm diameter was obtained. A Veeco MultiMode atomic force microscope (Veeco Instruments Inc, USA) with a silicon probe Tap300GD-G (Budget Sensors, USA) at a high aspect ratio tip (typical radius of curvature 10 nm) was used to image the surface of nanopaper in tapping mode at room temperature in an ambient atmosphere. The nanopaper thickness was measured by Hitachi SU-70 SEM scanning electron microscopy, performed using a Jeol JXA 840A system (Jeol Instruments, Tokyo, Japan) running at 5–10 keV. The optical properties of transmittance and haze of the nanopaper was obtained with a UV-Vis Spectrometer Lambda 35 (PerkInElmer, USA.), and the transmittance was measured between 1100 nm and 250 nm using a Shimadzu UV-Vis spectrometer.

Acknowledgements

We would like to thank the Biotechnology Research and Education Program for sharing the microfluidizer. L. Hu acknowledges the startup support from the University of Maryland College Park. We acknowledge the support of the Maryland Nanocenter and its Fablab and its Nisplab. The Nisplab is supported in part by the NSF as a MRSEC shared experimental facility.

References

1 K. N. Han, C. A. Li, M.-P. N. Bui and G. H. Seong, *Langmuir*, 2010, **26**, 598.
2 A. R. Rathmell and B. J. Wiley, *Adv. Mater.*, 2011, **23**, 4798.
3 W. J. Yu, S. Y. Lee, S. H. Chae, D. Perello, G. H. Han, M. Yun and Y. H. Lee, *Nano Lett.*, 2011, **11**, 1344.
4 V. Zardetto, T. M. Brown, A. Reale and A. Di Carlo, *J. Polym. Sci., Part B: Polym. Phys.*, 2011, **49**, 638.
5 S. Mecking, *Angew. Chem., Int. Ed.*, 2004, **43**, 1078.
6 L. Nyholm, G. Nystrom, A. Mihranyan and M. Stromme, *Adv. Mater.*, 2011, **23**, 3751.
7 A. N. Nakagaito, M. Nogi and H. Yano, *MRS Bull.*, 2010, **35**, 214.
8 M. C. Barr, J. A. Rowehl, R. R. Lunt, J. Xu, A. Wang, C. M. Boyce, S. G. Im, V. Bulovic and K. K. Gleason, *Adv. Mater.*, 2011, **23**, 3500.
9 E. Fortunato, N. Correia, P. Barquinha, L. Pereira, G. Goncalves and R. Martins, *IEEE Electron Device Lett.*, 2008, **29**, 988.
10 W. Lim, E. A. Douglas, S. H. Kim, D. P. Norton, S. J. Pearton, F. Ren, H. Shen and W. H. Chang, *Appl. Phys. Lett.*, 2009, **94**, 072103.
11 L. T. Fan, Y.-H. Lee and D. Beardmore, in *Advances in Biochemical Engineering*, Springer Berlin Heidelberg, 1980, vol. 14, p. 101.
12 M. Nogi, S. Iwamoto, A. N. Nakagaito and H. Yano, *Adv. Mater.*, 2009, **21**, 1595.
13 R. J. Moon, A. Martini, J. Nairn, J. Simonsen and J. Youngblood, *Chem. Soc. Rev.*, 2011, **40**, 3941.
14 I. Siro, D. Plackett, M. Hedenqvist, M. Ankerfors and T. Lindstrom, *J. Appl. Polym. Sci.*, 2011, **119**, 2652.
15 T. Saito, S. Kimura, Y. Nishiyama and A. Isogai, *Biomacromolecules*, 2007, **8**, 2485.
16 Z. H. Liu, X. J. Su, G. L. Hou, S. Bi, Z. Xiao and H. P. Jia, *J. Power Sources*, 2012, **218**, 280.
17 S. Brittman, H. W. Gao, E. C. Garnett and P. D. Yang, *Nano Lett.*, 2011, **11**, 5189.
18 B. T. Liu, Y. T. Teng, R. H. Lee, W. C. Liaw and C. H. Hsieh, *Colloids Surf., A*, 2011, **389**, 138.
19 Y. Habibi, L. A. Lucia and O. J. Rojas, *Chem. Rev.*, 2010, **110**, 3479.
20 A. Isogai, T. Saito and H. Fukuzumi, *Nanoscale*, 2011, **3**, 71.
21 C. H. Chung, T. B. Song, B. Bob, R. Zhu, H. S. Duan and Y. Yang, *Adv. Mater.*, 2012, **24**, 5499.
22 ASTM International, *Standard Test Method for Haze and Luminous Transmittance of Transparent Plastics*, West Conshohocken, PA, 2006, vol. D1003-11e1.
23 H. Fukuzumi, T. Saito, T. Wata, Y. Kumamoto and A. Isogai, *Biomacromolecules*, 2009, **10**, 162.
24 A. D. Liu, A. Walther, O. Ikkala, L. Belova and L. A. Berglund, *Biomacromolecules*, 2011, **12**, 633.
25 C. F. Bohren and D. R. Huffman, *Absorption and Scattering of Light by Small Particles*, Wiley, Hoboken, 1983.
26 L. Hu, G. Zheng, J. Yao, N. Liu, B. Weil, M. Eskilsson, E. Karabulut, Z. Ruan, S. Fan, J. T. Bloking, M. D. McGehee, L. Wågberg and Y. Cui, *Energy Environ. Sci.*, 2013, **6**, 513–518.
27 D. Felbacq, G. Tayeb and D. Maystre, *J. Opt. Soc. Am. A*, 1994, **11**, 2526.
28 S. Chandrasekhar, *Radiative Transfer*, Dover, Toronto, 1960.
29 K. Klier, *J. Opt. Soc. Am.*, 1972, **62**, 882.

